A COMPARISON OF A MICROSCOPIC AND A PHENOMENOLOGICAL

MODEL FOR A POLYATOMIC GAS

S. Körber, B. Wiesen
Fachbereich Mathematik
Universität Kaiserslautern
Postfach 3049
D - 6750 Kaiserslautern

A COMPARISON OF A MICROSCOPIC AND A PHENOMENOLOGICAL MODEL FOR A POLYATOMIC GAS

S. Körber and B. Wiesen

Department of Mathematics

University of Kaiserslautern

Abstract

Treating polyatomic gases in kinetic gas theory requires an appropriate molecule model taking into account the additional internal structure of the gas particles. In this paper we describe two such models, each arising from quite different approaches to this problem. A simulation scheme for solving the corresponding kinetic equations is presented and some numerical results related to 1 D shockwaves are compared.

0) Introduction

Due to the European Space research project HERMES there is a growing interest in the numerical solution of the Boltzmann-Equation, because this equation is the right one to describe the flow field around the shuttle during the phase of reentry where it moves down from attitudes over 150 km to about 70 km.

In such or other realistic situations simulation methods are by far the most important tools to solve the Boltzmann-Equation (see Nanbu's rewiew [9]). The first

of these schemes was proposed by Bird in 1968. It was based on the following philosophy:

Imitiate the behavior of the real gas molecules in a reduced particle system. In 1980 Nanbu proposed a new method directly related to the Boltzmann-Equation but suffering from practical weakness.

Starting from this point the laboratory of Technomathematics in Kaiserslautern has developed a simulation method which is now quite well understood and has proven to yield approximations of solutions of the Boltzmann-Equation given a sufficiently large number of test particles (for a review of this scheme see [7]).

The present paper deals with the extension of this algorithm to the case of gases with an internal structure. The treatment of these internal degrees of freedom can be done either from a phenomenological point of view or from a microscopic one. In the former case one concentrates on the exchange of energy between internal and kinetic modes. The rules for this exchange are generally found by physical heuristics and one has parameters at hand to fit computational results on experimental data.

Whereas such a procedure may be well motivated by practical reasons (e.g. to save computer time and storage) the situation remains still unsatisfactory. Therefore we have compared the by far mostly used phenomenological model [10] with a microscopic one.

The plan of the paper is as follows:

In the first chapter we describe our microscopic model and its collisional equations. Starting from these relations we derive the corresponding Boltzmann-Equation. To make the paper selfcontained we summarize the features of phenomenological models. In chapter 2 we introduce the Finite Pointset Method and describe the simulation algorithm. Chapter 3 shows the simulation results for a 1D shock wave. Chapter 4 gives a short summary.

I) Description of the Models

1. Description of a Microscopic Model for Polyatomic Gases

Considering a polyatomic gas one has to take into account the additional internal structure of the molecules. One approach to this problem is to consider only the internal energy due to these additional effects, described in the section below. The other approach is to construct a microscopic molecule model, which allows an explicit treatment of these inner effects. The model described in this paper only takes into account the additional rotational degrees of freedom, vibrational excitation is neglected.

One of the simplest models having rotational degrees of freedom is the so called 'loaded-sphere', which allows a rigorous analytical treatment while still retaining a large measure of geometric flexibility. This 'loaded-sphere'-model, first introduced by Jeans [1] into kinetic theory, is a spherical particle of radius a whose center of mass (M) is offset a distance ε from the geometric center (G) (see Figure 1). A molecule of this type is uniquely determined by its center-of-mass location x from a fixed origin, the linear velocity v, the angular velocity ω, and an unit orientation vector l directed along the axis of symmetry. Location of the surface with respect to the center of mass follows by defining the vector $\sigma(k) = \varepsilon l + a k$, k being the unit outward normal on the particle surface.
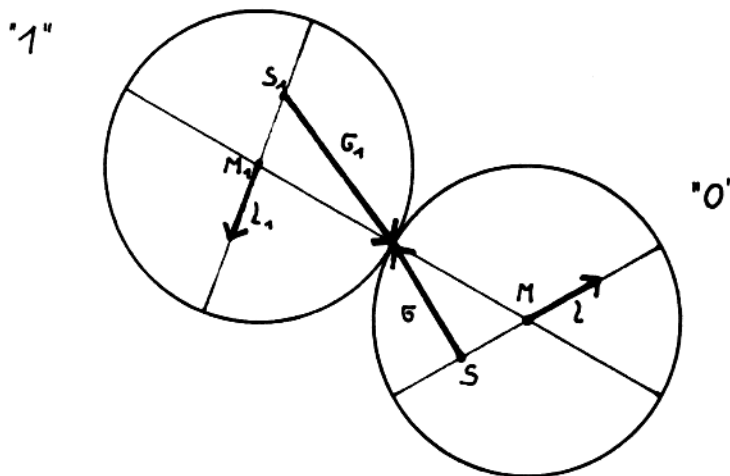

Figure 1

Under the assumption of binary collisions and molecular chaos one has the following:

A "0"-particle of mass m and moment of inertia Θ (with respect to the fixed origin) collides with an identical "1"-particle having precollision states $(x, v, \omega, 1)$ and $(x_1, v_1, \omega_1, 1_1)$, respectively, so that an impulse s is transmitted along the normal k to the particle surface at the impact point, k being positive outward from particle "0" (Figur 2). Since the collisions are instanteous, the location and orientation vectors remain unaltered during collision, and with primed postcollision quantities one has the following relations between pre- and postcollision variables from the equations of impact ([2], [3]):

Momentum 　　"0" : $m(v' - v) = - s \cdot k$

　　　　　　　　"1" : $m(v_1' - v_1) = s \cdot k$ 　　　　　　(1.1)

Angular Momentum 　"0" : $\Theta(\omega' - \omega) = - \sigma \times (s \cdot k)$

　　　　　　　　　　"1" : $\Theta(\omega_1' - \omega_1) = \sigma_1 \times (s \cdot k)$ 　　　(1.2)

Energy 　　$\frac{1}{2} m(v^2 + v_1^2) + \frac{1}{2} \Theta_{ij} \omega_i \omega_j + \frac{1}{2} \Theta_{ij} \omega_{i_1} \omega_{j_1}$

　　　　　　$= \frac{1}{2} m(v'^2 + v_1'^2) + \frac{1}{2} \Theta_{ij} \omega_i' \omega_j' + \frac{1}{2} \Theta_{ij} \omega_{i_1}' \omega_{j_1}'$ 　(1.3)

The transformation $(v, \omega, 1, v_1, \omega_1, 1_1) \rightarrow (v', \omega', 1', v_1', \omega_1', 1_1')$ is given by

$$v' = v - \frac{s}{m} \cdot k \qquad\qquad v_1' = v_1 + \frac{s}{m} \cdot k$$

$$\omega' = \omega - s \cdot \Theta^{-1} \cdot (\sigma \times k) \qquad \omega_1' = \omega_1 + s \cdot \Theta^{-1} \cdot (\sigma_1 \times k_1) \qquad (1.4)$$

$$1' = 1 \qquad\qquad 1_1' = 1_1$$

In these equations s is given by

$$s = \frac{- v \cdot k}{\frac{1}{m} + \frac{1}{2 I_1} (\sigma \times k)^2 + \frac{1}{2 I_1} (\sigma_1 \times k)^2} \qquad (1.5)$$

where

$$\nu = \left(v_1 - v + \omega_1 \times \sigma_1 - \omega \times \sigma \right) \tag{1.6}$$

defines the relative velocity of the impact points before collision and I_1 is the moment of inertia about an axis perpendicular to the axis of symmetry l. With $\sigma = \varepsilon l + a k$ equations (1.5) and (1.6) turn into:

$$S = \frac{-\nu \cdot k}{\frac{1}{m} + \frac{1}{2 I_1} \varepsilon^2 (l \times k)^2 + \frac{1}{2 I_1} \varepsilon^2 (l_1 \times k)^2} \tag{1.7}$$

$$\nu = \left(v_1 - v + \varepsilon (\omega_1 \times l_1) - \varepsilon (\omega \times l) \right) \tag{1.8}$$

For the polyatomic 'loaded-sphere'-model the state of such a particle involves the location and the translational velocity as well as the angular velocity and the orientation. One therefore defines the state space Γ involving all possible states and consisting of the location space $\Lambda \subset \mathbb{R}^3$, the velocity space $V = \mathbb{R}^3$, the angular velocity space $\Omega = \mathbb{R}^3$ and the orientation space $O = S^2$ (unit sphere), i.e.

$$\Gamma = \Lambda \times V \times \Omega \times O = \Lambda \times \mathbb{R}^3 \times \mathbb{R}^3 \times S^2$$

A distribution function $f \in L^1_+ (\Gamma)$ is defined in such a way that $f(t, x, v, \omega, l) dx \, d\tau$ denotes the number of particles in the configuration element $dx \, d\tau = dx \, dv \, d\omega \, dl$. A region Σ_0 in the state space Γ at time $t_0 = 0$ maps into a region $\Sigma_t = T_t \Sigma_0$ in time, where T_t is the free flow operator which will be discussed later. Particles originally in Σ_0 will be in Σ_t at time t unless their trajectories are altered by collision. This statement leads up to

$$\frac{d}{dt} \int\limits_{\Sigma_t} f \, dx \, dv \, d\omega \, dl = \int\limits_{\Sigma_t} J(f, f) \, dx \, dv \, d\omega \, dl \tag{1.9}$$

where $J(f, f)$ denotes as usual the collision term.

Provided a sufficient smooth distribution function f one obtains by applying a transport theorem the following polyatomic Boltzmann-Equation

$$\frac{\partial f}{\partial t} + \frac{\partial f}{\partial x} \dot{x} + \frac{\partial f}{\partial v} \dot{v} + \frac{\partial f}{\partial \omega} \dot{\omega} + \frac{\partial f}{\partial l} \dot{l} = J(f, f) \tag{1.10}$$

Representing the orientation vector – distributed over the unit sphere – by the corresponding polar angles φ_1 and φ_2 ($\varphi_1 \in [0, 2\pi)$; $\varphi_2 \in [0, \pi]$), equation (1.10) reads

$$\frac{\partial f}{\partial t} + \frac{\partial f}{\partial x} \dot{x} + \frac{\partial f}{\partial v} \dot{v} + \frac{\partial f}{\partial \omega} \dot{\omega} + \left(\frac{\partial f}{\partial \varphi_1} \dot{\varphi}_1 + \frac{\partial f}{\partial \varphi_2} \dot{\varphi}_2 \right) = J(f, f) \qquad (1.11)$$

To introduce the free flow operator we have to discuss the equations of motion of a free particle are (NEWTON – Equations)

$$\dot{x} = v$$
$$\dot{v} = F \ (\text{force/mass}) \qquad (1.12)$$

For discussing the rotational motion it is convienient to introduce a coordinate system with the center of mass as origin and the axis along the main axis of inertia. In this system the equation of rotational motion are given by the EULER-Equations

$$I_1 \dot{\omega}_1 = \omega_2 \omega_3 (I_1 - I_2)$$
$$I_1 \dot{\omega}_2 = - \omega_1 \omega_3 (I_1 - I_2) \qquad (1.13)$$
$$I_2 \dot{\omega}_3 = 0$$

where I_2 , I_1 are the moments of inertia in this system about the 1 – axis and an axis perpendicular to 1, respectivly. Equation (1.13) is equivalent to the vector equation

$$\dot{\omega} = \frac{I_1 - I_2}{I_1} \omega_3 (\omega \times 1) = \frac{I_1 - I_2}{I_1} \langle \omega, 1 \rangle (\omega \times 1) \qquad (1.14)$$

The time derivative of the orientation vector is given by

$$\dot{1} = \omega \times 1 \qquad (1.15)$$

or in terms of the corresponding polar angles φ_1 and φ_2

$$\dot{\varphi}_i = \left\langle \omega \times 1, \alpha_i \frac{\partial 1}{\partial \varphi_i} \right\rangle \qquad i = 1,2$$

with

$$\alpha_1 \frac{\partial 1}{\partial \varphi_1} \ , \quad \alpha_2 \frac{\partial 1}{\partial \varphi_2} \qquad \left(\alpha_1 = \frac{1}{\sin \varphi_2} \ , \quad \alpha_2 = 1 \right)$$

being an orthonormalbasis in the tangential plane to the unit sphere determined by the orientation vector 1 .

If we denote the state space of a single particle by $\vec{Z} = (x, v, \omega, 1)$ then we have because of the global existence of solutions of (1.12), (1.14) and (1.15) for reasonable forces a well defined free operator T_t which simply maps the initial state $\vec{Z}_0$ to the state at time t.

Combining the results in (1.11), (1.12), (1.14) and (1.15) one ends up with the Boltzmann-Equation of the following form

$$\frac{\partial f}{\partial t} + v \frac{\partial f}{\partial x} + F \frac{\partial f}{\partial v} + \frac{I_1 - I_2}{I_1} \langle \omega, 1 \rangle (\omega \times 1) \frac{\partial f}{\partial \omega} + \langle \omega \times 1, \alpha_i \frac{\partial 1}{\partial \varphi_i} \rangle \frac{\partial f}{\partial \varphi_i} = J(f, f)$$

On the left the first three terms make up the streaming portion of the monoatomic Boltzmann-Equation while remaining three terms are related to the polyatomic structur of the 'loaded-sphere' model.

Since the transformation (1.4) is its own inverse the right hand sided collision term can be derived in the same fashion as in the monoatomic case, resulting

$$J(f, f) = \int_{\langle v, k \rangle > 0} |\langle v, k \rangle| \times f(\tau') f(\tau_1') \, d\mu(k) \, d\tau_1 - \int_{\langle v, k \rangle < 0} |\langle v, k \rangle| \times f(\tau) f(\tau_1) \, d\mu(k) \, d\tau_1$$

$$\tau = (v, \omega, 1)$$

Here $\times$ denotes the differential cross section which is in the case of 'loaded spheres' the same as for hard spheres, i.e.

$$\times = 4 a^2$$

Since the collision equations (1.4) are symmetric in k one ends up with the Boltzmann-Equation for 'loaded-spheres' given in the following way $\left(\Pi = \mathbb{R}^3 \times \mathbb{R}^3 \times S^2 \right)$:

$$\frac{\partial f}{\partial t} + v \frac{\partial f}{\partial x} + F \frac{\partial f}{\partial v} + \frac{I_1 - I_2}{I_1} \langle \omega, 1 \rangle (\omega \times 1) \frac{\partial f}{\partial \omega} + \langle \omega \times 1, \alpha_i \frac{\partial 1}{\partial \varphi_i} \rangle \frac{\partial f}{\partial \varphi_i} \qquad (1.16)$$

$$= \frac{1}{2} \int_{\Pi} \int_{S^2} |\langle v, k \rangle| \times \left(f(\tau') f(\tau_1') - f(\tau) f(\tau_1) \right) d\mu(k) \, d\tau_1$$

2. The Kinetic Equation for Phenomenological Models

In many cases one is not interested in the details of the evolution of the internal coordinates but in the exchange of internal and translational energy. In such a situation the complete simulation is by far to expensive. For this reason phenomenological equations are introduced in which this energy exchange is controlled by models which are based on physical heuristics and which have parameters to fit computational results and experimental data. the kinetic equation which gives the mathematical framework to study such models is [6]

$$\left(\frac{\partial}{\partial t} + v \frac{\partial}{\partial x} \right) f(t,x,v,\varepsilon) \tag{1.17}$$

$$= \int_{\mathbb{R}^3} \int_{\mathbb{R}_+} \int_{\Delta_E} \int_{S^2} \| v - w \| \ \sigma \left(E \, ; \, \varepsilon, \varepsilon_1 \to \varepsilon', \varepsilon_1' \, ; \eta \cdot \eta' \right) \left(f' \cdot f_*' - f \cdot f_* \right) \, d\mu(\eta') \, d^2\varepsilon' \, d^2\varepsilon_1 \, d^3w$$

with

$$E = \frac{m}{4} \| v - w \|^2 + \varepsilon + \varepsilon_1$$

$$v' = \frac{1}{2} \left((v + w) + \eta' \sqrt{\frac{4}{m}(E - \varepsilon' - \varepsilon_1')} \right)$$

$$f = f(t,x,v,\varepsilon) \qquad\qquad f_* = f(t,x,w,\varepsilon_1)$$

$$f' = f(t,x,v',\varepsilon') \qquad\qquad f_*' = f(t,x,w',\varepsilon_1')$$

$$\Delta_E = \left\{ (\varepsilon',\varepsilon_1') \, : \, 0 \le \varepsilon', \varepsilon_1' \, ; \, \varepsilon' + \varepsilon_1' \le E \right\}$$

As can be seen by inspection of the left hand side of (1.17) the free flow operator takes here a particularly simple form:

Denoting by $\vec{z} = (x,v,\varepsilon)$ we have

$$T_t(\vec{z}) = (x + tv, v, \varepsilon) \tag{1.18}$$

In (1.17) the different models for the energy exchange are described by specific σ 's. The by far most famous model is the so called *Larsen-Borgnakke* model. For this model the scattering cross-section reads

$$\sigma(E; \varepsilon, \varepsilon_1 \to \varepsilon', \varepsilon_1'; \eta \cdot \eta')$$

$$= Z(E) \sigma_o(\|v - w\|) h(\eta \cdot \eta') \delta(\varepsilon - \varepsilon') \delta(\varepsilon_1 - \varepsilon_1')$$

$$+ (1 - Z(E)) \sigma_o(\|v - w\|) R(E; \varepsilon, \varepsilon_1 \to \varepsilon', \varepsilon_1') h(\eta \cdot \eta')$$

with

$$\int_{S^2} h(\eta \cdot \eta') \, d\mu(\eta') = 1 \qquad \int_{\Delta_E} R \, d^2\varepsilon' = 1$$

$$R = \sigma_o(\|v' - w'\|) \|v' - w'\|^2 N(E)$$

The features of this model are

- The total cross section depends on $\|v - w\|$ only.
- A part of the collisions is elastic. The ratio of elastic to inelastic collisions is controlled by the total collision energy.
- The 'energy scattering kernel' does not depend on ε or ε_1; it is determined by the total cross section σ_o.

II) The Finite Pointset Method (FPM)

In this section we will describe how the ideas of the FPM described in [7] can be transformed for the case of internal energy models. To get an approximation of the solution of the Boltzman-Equation by point measures (particle simulation) one has to perform the following steps:

a) time discretization

b) separation of 'free flow' and interaction

c) local homogenization

d) weak formulation

e) measure formulation

To do so we first rewrite the Boltzmann-Equation in its so called mild formulation

$$\frac{d}{dt} f(t, T_t(\vec{z})) = J(f, f)(T_t(\vec{z})) \tag{2.1}$$

Here T_t is the free flow operator described in section one (see (1.12), (1.14), (1.15) and (1.18) respectively) and $\vec{z}$ is the state vector of the system under consideration. If we approximate the derivative on the left hand side by a difference quotient we obtain easily a first order approximation of the solution given by a sequence of recursively defined functions:

$$f_{n+1}(T_{\Delta t}(\vec{z})) = f_n(\vec{z}) + \Delta t\, J(f_n, f_n)(\vec{z}) \tag{2.2}$$

From section one we have seen the following properties of T_t and the collision operator J

a) in the case of the microscopic model:

   T_t does not change velocities and if the initial angular velocity is perpendicular to the orientation vector it is also unchanged. These quantities are changed due to collisions in which the orientation of the particles enters as a parameter.

b) in the case of the phenomenological model:

   The free flow changes the position; the collisions change the velocities and the internal energy.

These properties together with the particular form of (2.2) suggest to split the iteration formula into two steps:

the _collision_ simulation

$$g_{n+1}(\vec{z}) = f_n(\vec{z}) + \Delta t\, J(f_n, f_n)(\vec{z}) \tag{2.3}$$

and the _free flow_

$$f_{n+1}(\vec{z}) = g_{n+1}(T_{-\Delta t}(\vec{z})) \tag{2.4}$$

The numerical simulation of (2.4) will be obvious. So we have to concentrate on (2.3). Notice that (2.3) is a discretized version of the spatially homogeneous Boltzmann-Equation.

To handle the collision process - in which the space coordinate is unchanged - we have to introduce the concept of spatial homogenization according to a given cell structure. To do this we divide the domain of computation Λ into cells:

$$\Lambda = \bigcup C_i \qquad C_i \cap C_j = \emptyset \qquad i \neq j \qquad i,j = 1, \ldots, M$$

and introduce the homogenization operator

$$f(x, \_) \mapsto \sum_{i=1}^{M} \chi_{c_i}(x) \frac{1}{\lambda^3(C_i)} \int_{c_i} f(x', \_) dx' \qquad (2.5)$$

Here $\chi_{c_i}(x)$ is the characteristic function of the cell C_i. From (2.4) it can be seen that the free flow destroys this homogenization so that it has to be performed before each collision step.

Now we tackle the main question of the simulation, namely the performance of the collisions. In the case of phenomenological models this procedure has been described in great detail in [6] so that we concentrate on the case of the microscopic model. Because the principles of the collision simulation are the same for each cell, we can simplify the notation: we denote by $f_j(v,\omega,1)$ the homogenized density function in an arbitrary but fixed cell at time $j \cdot \Delta t$. Then equation (2.3) reads:

$$f_{j+1}(\tau) = \left(1 - \Delta t \frac{1}{2} \int_{\Pi} \int_{S^2} |\langle v, k \rangle| \times f_j(\tau_1) \, d\mu(k) \, d\tau_1 \right) f_j(\tau)$$

$$+ \Delta t \frac{1}{2} \int_{\Pi} \int_{S^2} |\langle v, k \rangle| \times f_j(\tau') f_j(\tau_1') \, d\mu(k) \, d\tau_1 \qquad (2.6)$$

Here τ denotes $(v,\omega,1)$ as in section one. As can be seen from (2.6) the requirement that f_{j+1} is a nonnegative function forces a truncation of the collision kernel $|\langle v, k \rangle| \times$. Fortunately, in practical cases this can be done in a way that only a few particles are affected.

In a next step we renormalize the density function, i.e. we replace f_j by

$$f_j \longrightarrow f_j \Big/ \int_{C_i} \int_\Pi f_j(\tau)\, d\tau\, dx$$

This renormalization gives an additional term to the scattering cross section x:

$$x \longrightarrow x \int_{C_i} \int_\Pi f_j(\tau)\, d\tau\, dx$$

Having prepared (2.6) in this way we may proceed to the weak formulation of this equation: we multiply (2.6) with a test function $\varphi \in C_b(\Pi)$, integrate, and use the fact that the collision maps to its own inverse:

$$\int_\Pi f_{j+1}(\tau)\, \varphi(\tau)\, d\tau = \int_{\Pi \times \Pi} \left[k(\tau,\tau_1)\varphi \right] f_j(\tau)\, f_j(\tau_1)\, d\tau\, d\tau_1 \qquad (2.7)$$

Here we have:

$$\left[k(\tau,\tau_1)\varphi \right] = \int_0^1 \int_{S^2} \varphi\left(\tilde{\tau}(\alpha,k;\tau,\tau_1) \right)\, d\tilde{\mu}(k)\, d\alpha$$

with

$$\tilde{\tau}(\alpha,k;\tau,\tau_1) = \begin{cases} \tau'(k;\tau,\tau_1) & \alpha \le \frac{1}{2}\int_{S^2} |\langle v, k\rangle|\, x\, d\mu(k) \\[2mm] \tau & 1 > \alpha > \frac{1}{2}\int_{S^2} |\langle v, k\rangle|\, x\, d\mu(k) \end{cases}$$

and

$$d\tilde{\mu}(k) = \left[\frac{1}{2}\int_{S^2} |\langle v, k\rangle|\, x\, d\mu(k) \right]^{-1} \cdot \frac{1}{2} |\langle v, k\rangle|\, x\, d\mu(k) \qquad (2.8)$$

Equation (2.7) together with (2.8) is of standard type, which has been discussed in other papers ([6],[8]), and its measure theoretic interpretation is now straightforward:

Suppose you have a discrete approximation μ_j^N of the density function:

$$\mu_j^N = \frac{1}{N} \sum_{i=1}^N \delta(\tau - \tau_{ji}^N)$$

such that $\mu_j^N \xrightarrow{\text{w}} f_j(\tau)\,d\tau$. How to find a corresponding sequence of discrete probability measures μ_{j+1}^N with $\mu_{j+1}^N \xrightarrow{\text{w}} f_{j+1}(\tau)\,d\tau$?

One possible way to do this will be described by the following algorithm:

Suppose you have N point measures $\tau_1 \ldots \tau_N$.

1) Choose randomly a permutation p of $\{1 \ldots N\}$ and group together $\frac{N}{2}$ pairs:

$$(\tau_{\pi(1)}, \tau_{\pi(2)}) \, , \, (\tau_{\pi(3)}, \tau_{\pi(4)}) \, , \, \ldots$$

2) For each pair of these pairs $(\tau_{\pi(i)}, \tau_{\pi(i+1)})$ generate a $[0,1]$ uniformly distributed random number α and a random unit vector distributed according $d\tilde{\mu}(k)$.

IF $\quad \alpha \leq \frac{1}{2}\int_{S^2} |<v, k>| \times d\mu(k))$

$$S \quad \longleftarrow \quad \frac{-v \cdot k}{\frac{1}{m} + \frac{1}{2\,I_1}\varepsilon^2\left(1_{\pi(i)} \times k\right)^2 + \frac{1}{2\,I_1}\varepsilon^2\left(1_{\pi(i+1)} \times k\right)^2}$$

$$v_{\pi(i)} \quad \longleftarrow \quad v_{\pi(i)} - \frac{S}{m} \cdot k$$

$$v_{\pi(i+1)} \quad \longleftarrow \quad v_{\pi(i+1)} + \frac{S}{m} \cdot k$$

$$\omega_{\pi(i)} \quad \longleftarrow \quad \omega_{\pi(i)} - s \cdot \Theta^{-1} \cdot (\sigma \times k)$$

$$\omega_{\pi(i+1)} \quad \longleftarrow \quad \omega_{\pi(i+1)} + s \cdot \Theta_1^{-1} \cdot (\sigma_1 \times k)$$

ENDIF

Recall that in (2.9) the relative velocity of the points of impact is dependent on $\tau_{\pi(i)}, \tau_{\pi(i+1)}$. Θ and Θ_1 are the inertia tensors dependant on $1_{\pi(i)}, 1_{\pi(i+1)}$ and σ and σ_1 are given by

$$\sigma = \varepsilon 1_{\pi(i)} + a\,k \qquad \sigma_1 = \varepsilon 1_{\pi(i+1)} + a\,k$$

From the formula in (2.9) it is obvious that in this algorithm linear momentum, angular momentum and energy are conserved in each collision.

Another fact which is important from the numerical point of view is that this is very easily to implement in a completly vectorized manner.

III) One-Dimensional Shockwaves

After having introduced two quite different models describing a polyatomic gas in the previous sections, we will now apply these models and the corresponding simulation schemes to a classical problem arising in gas motion, namely the internal structure of a shockwave. To simulate such a shockwave we assume that the gas is far off the shockfront in equilibrium. These equilibrium states will be described via the quantities ρ_i, T_i, u_i denoting the density, temperature and velocity, where $i = 1$ indicates the upsteam and $i = 2$ the downstream. A characteristic lenght is introduced by the shockthickness Δ defined by (Figure 2):

$$\Delta := \frac{\rho_2 - \rho_1}{\left(\frac{d\rho}{dx}\right)_{max}}$$
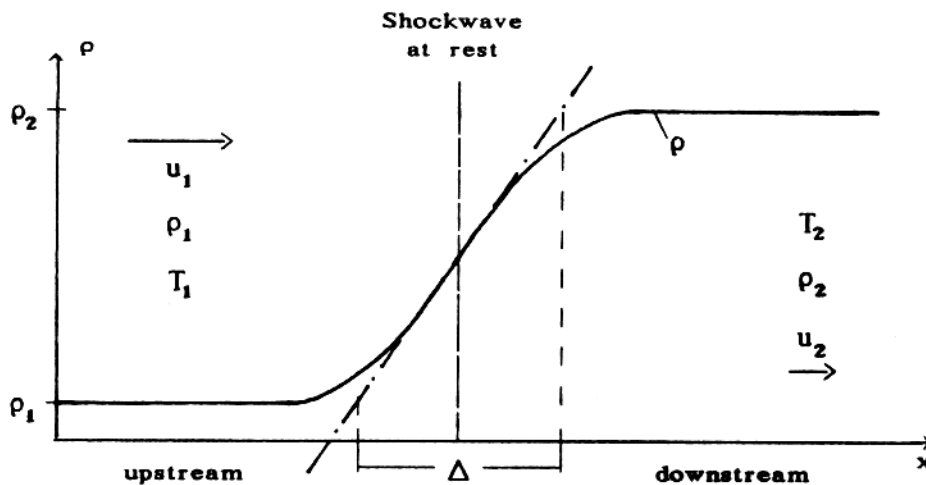
Figure 2

In the following we will restrict to an onedimensional planar shockwave, which advances along the spatially x-axis (this can be achieved by rotating the coordinate system), i.e. the shockwave is independant of the remaining coordinates. Furthermore we set external forces to zero and assume that the moving gas is in an equilibrium state far upstream and downstream. Refering to a coordinate system with the shockwave at rest we can write down the conditions related to the conservation of mass, momentum and energy while crossing the shockwave, i.e.

mass
$$\rho_1 \cdot u_1 = \rho_2 \cdot u_2$$

momentum
$$\rho_1 \cdot u_1^2 + p_1 = \rho_2 \cdot u_2^2 + p_2 \tag{3.1}$$

energy
$$\rho_1 \cdot u_1 \left(\frac{1}{2} u_1^2 + \frac{5}{2} R T_1 \right) + p_1 \cdot u_1 + q_1 = \rho_2 \cdot u_2 \left(\frac{1}{2} u_2^2 + \frac{5}{2} R T_2 \right) + p_2 \cdot u_2 + q_2$$

In these equations we used the additional notations: p pressure, q heatflux.

In the far off equilibrium one has the following conditions concerning the pressure and the heatflux:

$$p_i \rightarrow p_{i\infty} = \rho_i R T_i$$
$$q_i \rightarrow q_{i\infty} = 0$$

$$i = 1,2$$

Hence (3.1) can be reduced to

$$\rho_1 \cdot u_1 = \rho_2 \cdot u_2$$

$$\rho_1 \cdot u_1^2 + \rho_1 R T_1 = \rho_2 \cdot u_2^2 + \rho_2 R T_2 \tag{3.2}$$

$$\frac{1}{2} u_1^2 + \frac{7}{2} R T_1 = \frac{1}{2} u_2^2 + \frac{7}{2} R T_2$$

The equations (3.2) are the well known Rankine-Hugoniot-conditions in term of a polyatomic gas.

Representating the shock profiles one usually relates to the normalized quantities for density and temperatur ($\overline{\rho}$, $\overline{T}$) defined by

$$\overline{\rho} = \frac{\rho - \rho_1}{\rho_2 - \rho_1} \qquad \overline{T} = \frac{T - T_1}{T_2 - T_1}$$

In terms of these quantities one obtains the well known shock profile shown below in Figur 3.
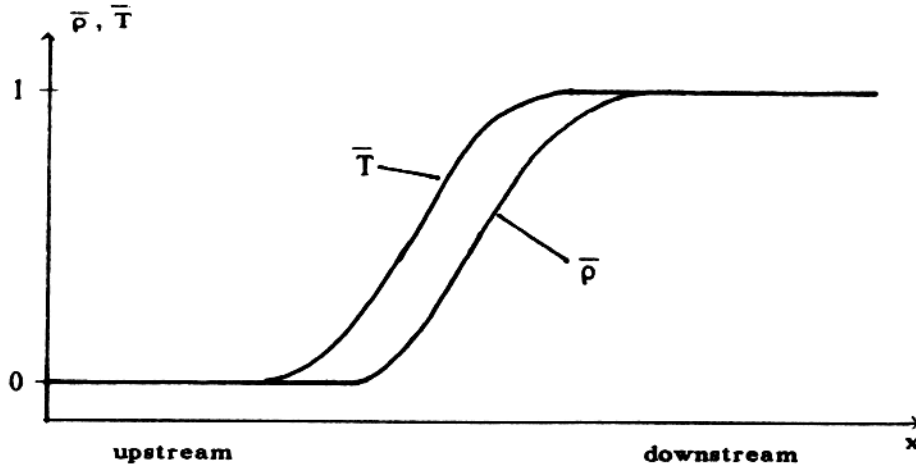
$\bar{\rho}, \bar{T}$

Figure 3

Considering a polyatomic gas one has to take into account the additional phenomena arising from the different degrees of freedom. While passing the shock the gain of energy occurs in two steps. First there is a narrow region where the fast degrees of freedom gain energy while the slow degrees remain inert. Then there is a broader relaxion zone involving a gradual approach to equilibrium between all degrees of freedom. In the present models the fast degrees are due to translation and the slower degrees are due to rotation. Representating these different types of energy with the corresponding temperatures one gets the following qualitative structure:

$\bar{T}_T, \bar{T}_R$
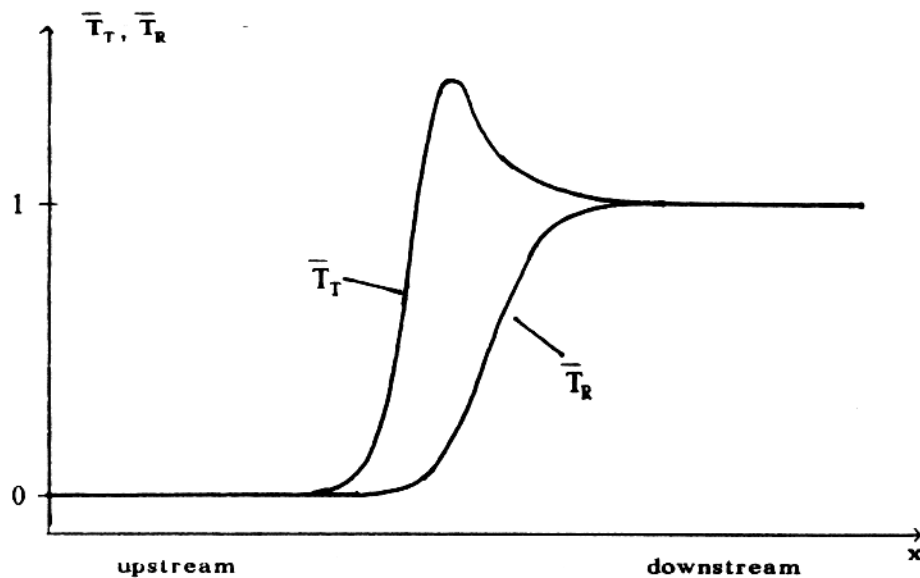
Figure 4

A parameter describing the transition ratio between translational and inner energy in the case of the phenomenological model is easily found and given by the *collision rate*.

In case of the 'loaded spheres' it is obvious that the transition between the translational and the rotational (= internal) energy is dependant of the eccentricity, which describes the geometric variation of the loaded spheres from the hard spheres. In this case an appropriate parameter γ is motivated by the transformation equations (1.4) and given by

$$\gamma(\epsilon) = \frac{\epsilon}{i(\epsilon)} \qquad (3.3)$$

with $i(\epsilon)$ being the radius of inertia (see [2],[3]). Decreasing values of γ cause a smaller transition between the two forms of energy, i.e. the relaxation zone until the downstream equilibrium is reached tends to infinity. Realize that $\gamma = 0$ equals the hard sphere and that in this case there is no energy transition. While crossing the shock only the translational energy is altered, the rotational energy remains unaltered, i.e. the relaxation zone is infinity.

When the 'loaded-sphere' does not differ much from the hard-sphere (small ϵ) then the transition parameter γ is nearly linearly dependant on the eccentricity (compare Figure 5).
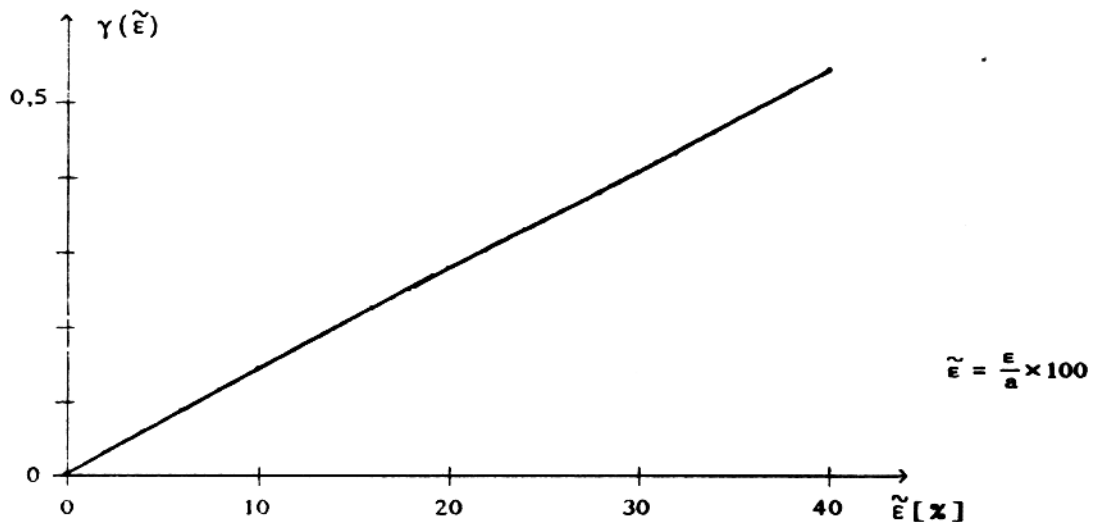
Figure 5

Below we show 5 plots of an internal structure of a one-dimensional shock wave resulting from the simulation process described in the previous section done on a Siemens VP100 vector computer. Here we restrict on a upstream velocity of 20 Ma, for other Mach-Numbers consult [3]. Due to a limit in CPU seconds it was not possible to receive shockwave profiles for eccentricities less than 5%. The corresponding CPU-time on the vector unit were

| Eccentricity $\tilde{\epsilon}$ %		5	7,5	10	15	20
CPU-Time	min	40	32	25	19	14

The numerical results shown in the figures are quite similar to experimental measurements [5]. The sharp bend in the density and temperature curve before reaching the downstream equilibrium is a typical phenomena while using Boltzmann simulation schemes, but are considered more realistic than the symmetric Navier-Stokes solutions (see [4]). Note that with increasing eccentricity the rotational temperature leaves the upsteam equilibrium earlier and even starts to increase sooner than the density when increasing the eccentricity even more.
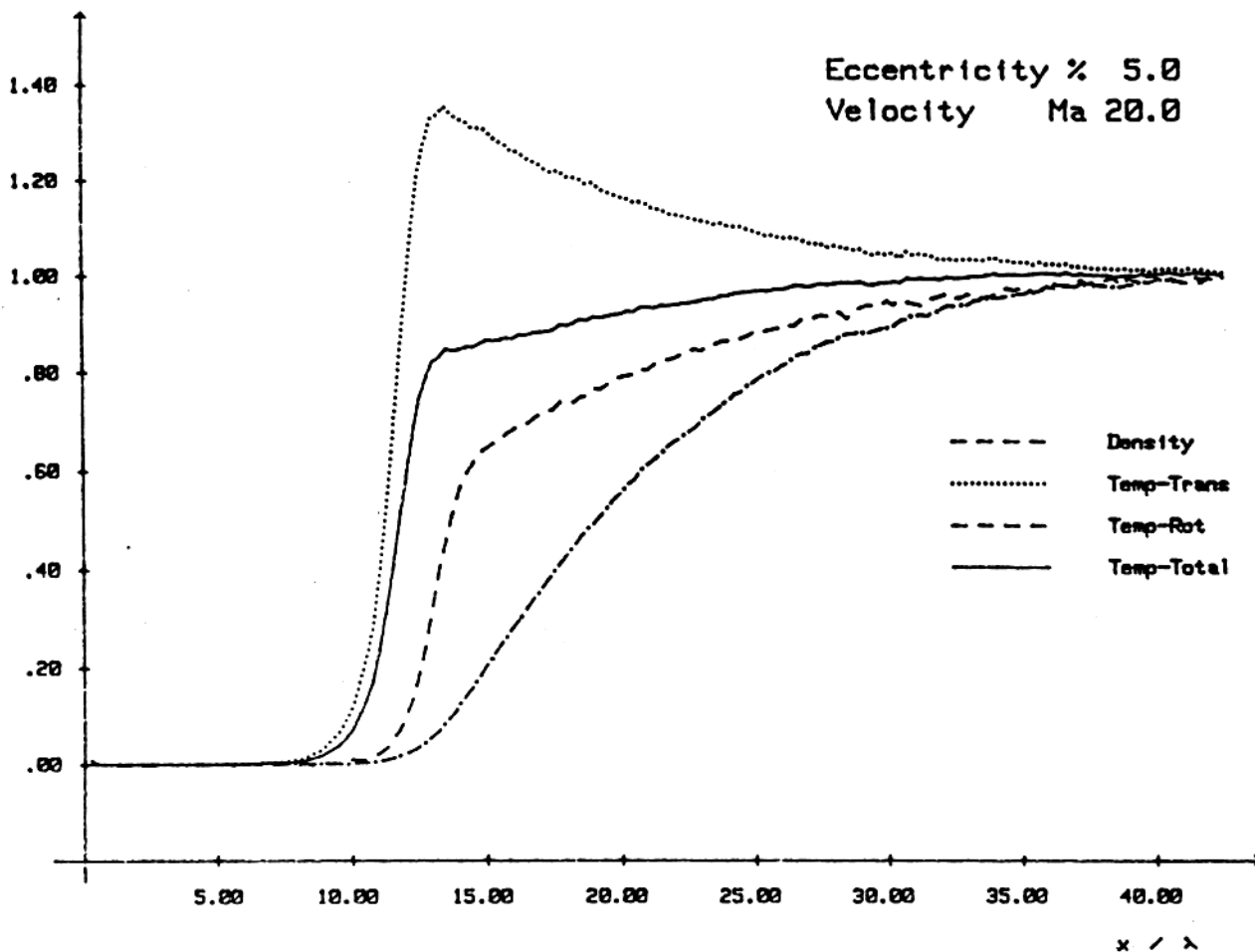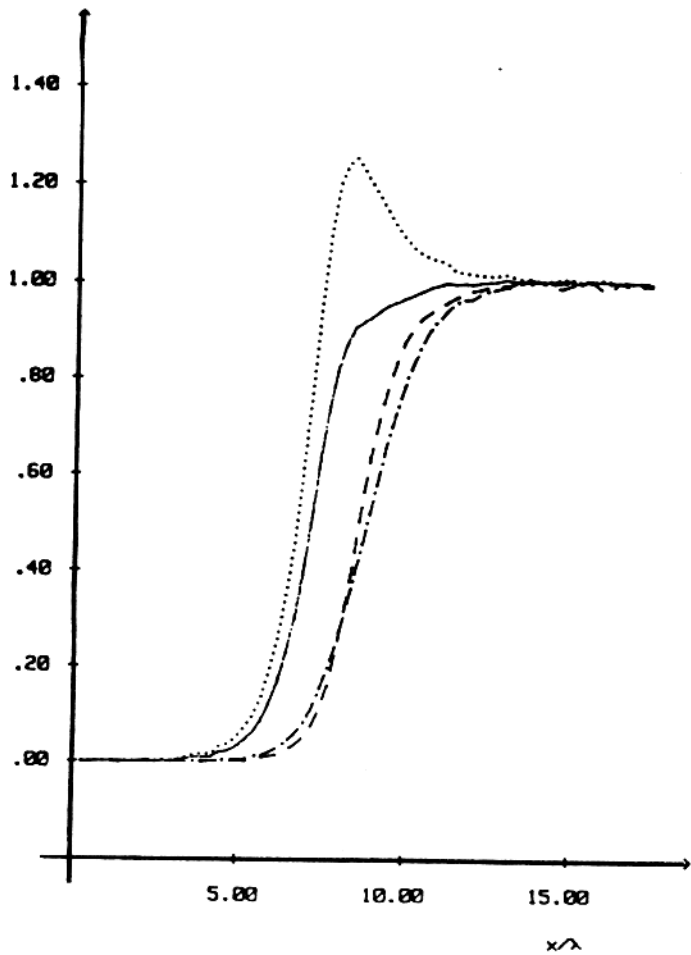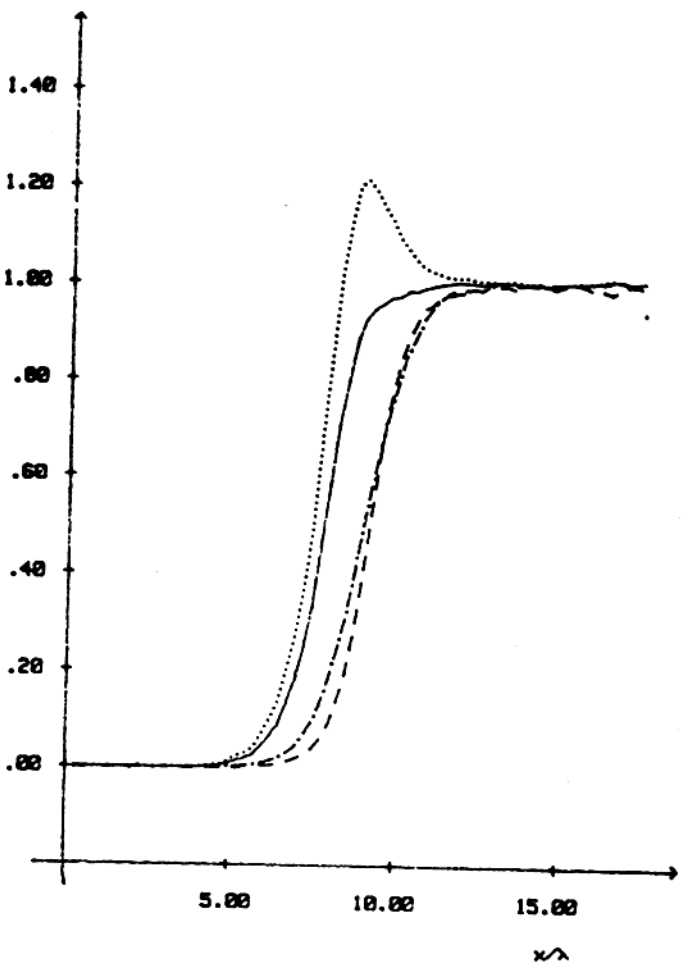
Eccentricity % 15.0
Velocity   Ma 20.0
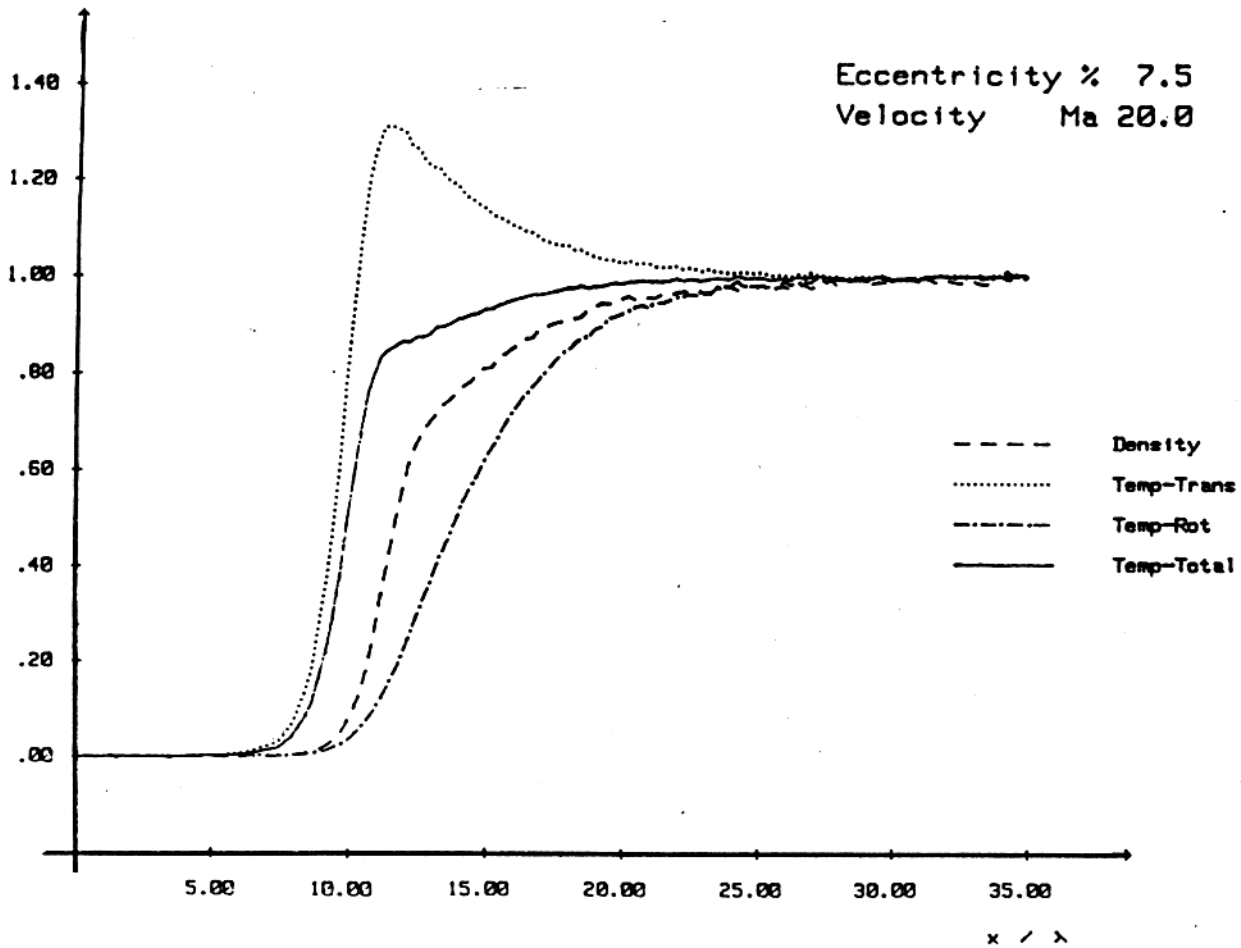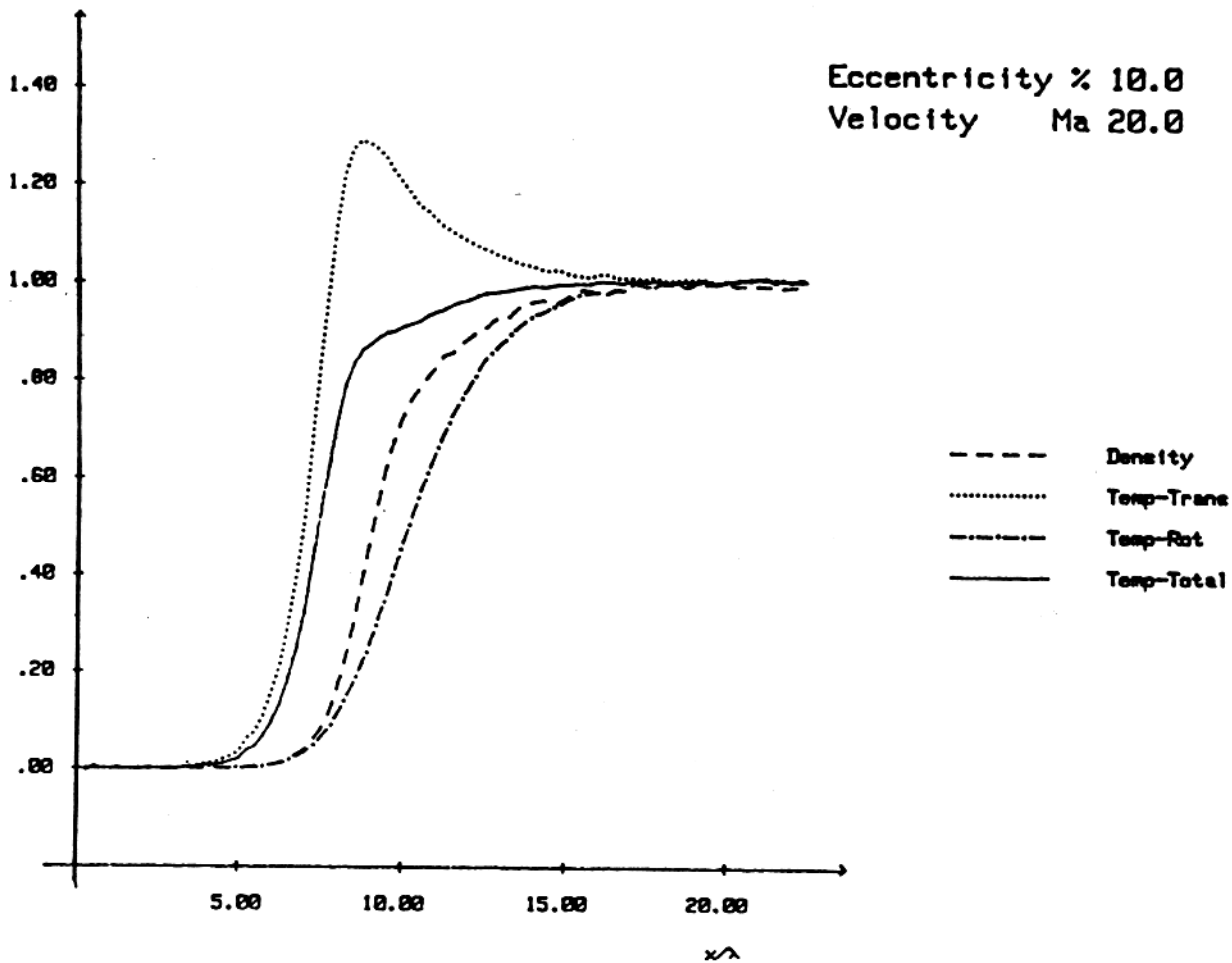
- - - -   Density
....   Temp-Trans
-·-·-   Temp-Rot
——   Temp-Total

Eccentricity % 20.0
Velocity   Ma 20.0

- - - -   Density
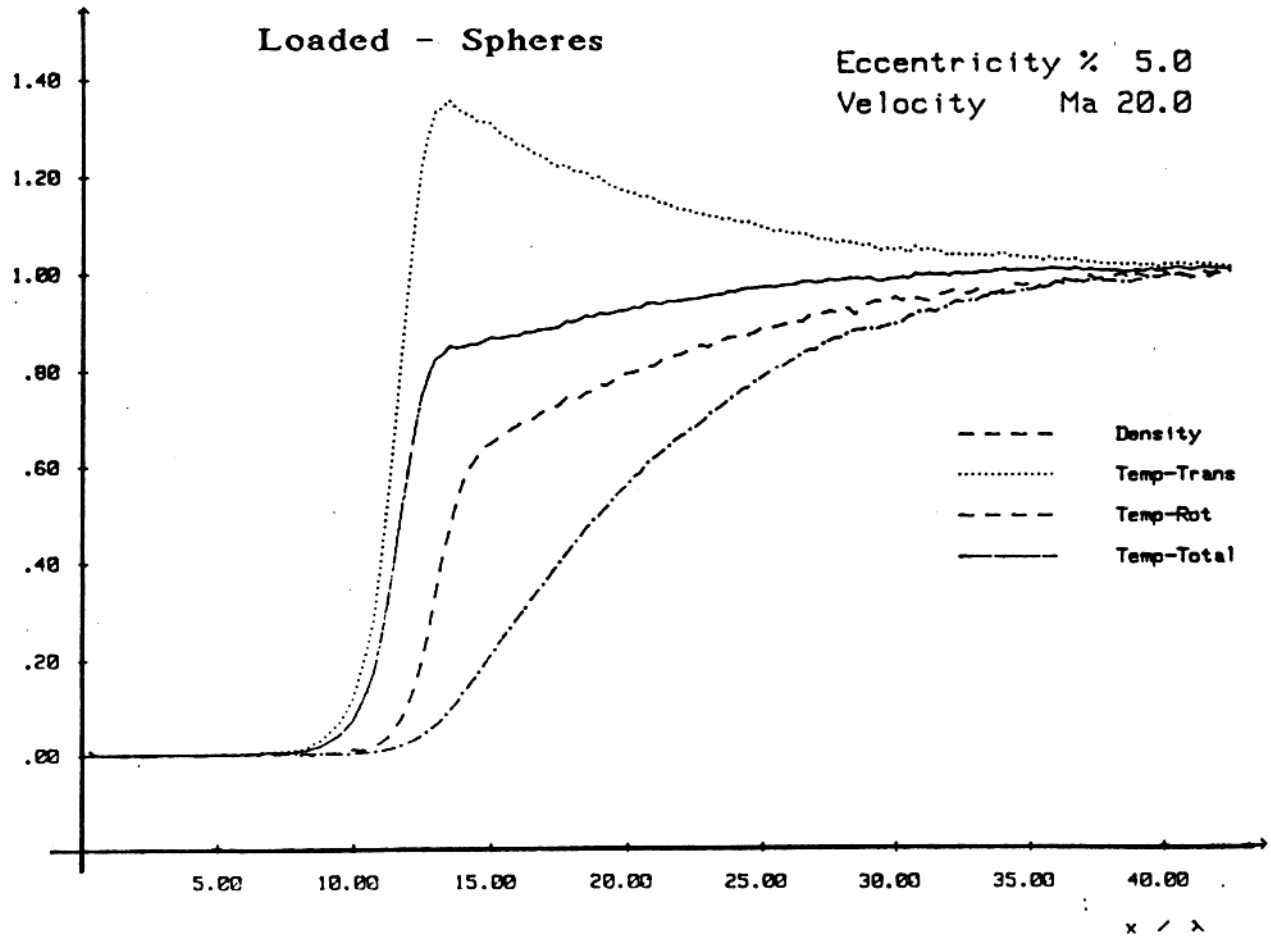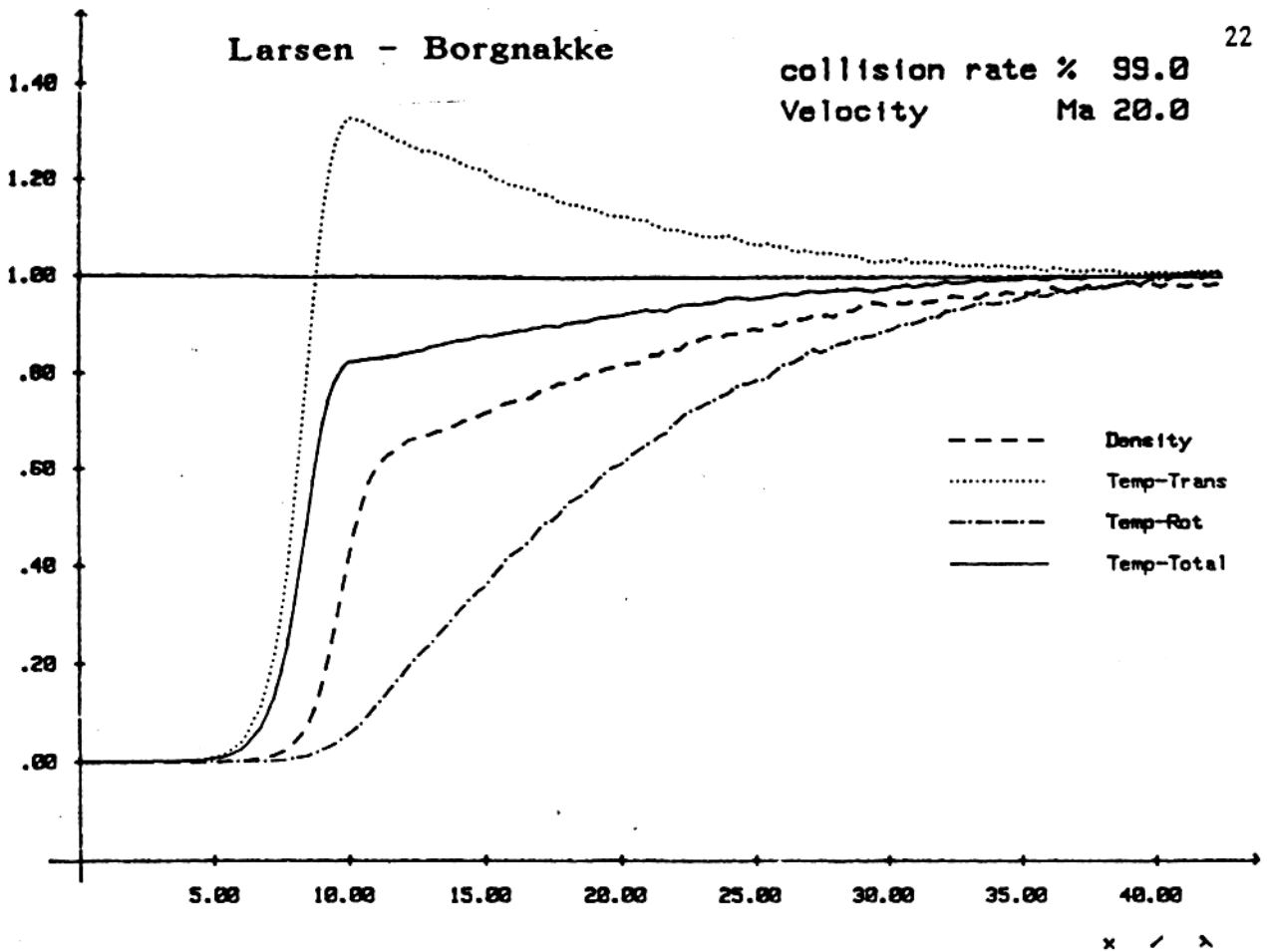.........   Temp-Trans
-·-·-   Temp-Rot
——   Temp-Total

In order to compare these two models describing a polyatomic gas in a quite different way, one has to care for an appropriate criterion. Refering to the internal structure of a shockwave the density and temperature profiles are mainly dependent on the transition rate between the two different kinds of energies. By examining the impact equations (1.4) – (1.8) for the 'loaded-sphere' model it follows directly that the ratio of transition between translational and internal (rotational) energy is proportional to the square of $\gamma(\varepsilon)$ (see (3.3)), while this ratio in case of the phenomenological model is given by the collision rate. Thus we have:
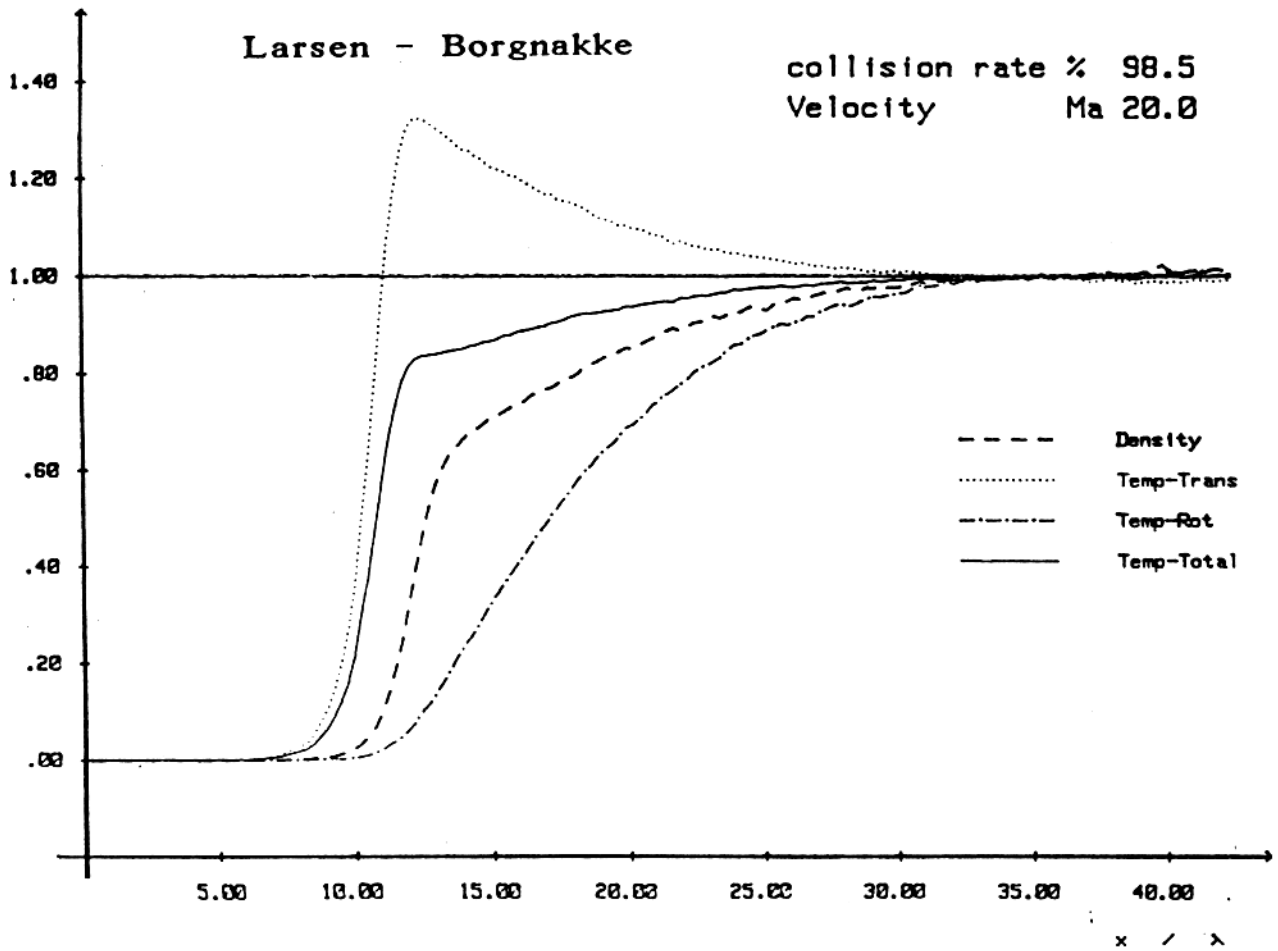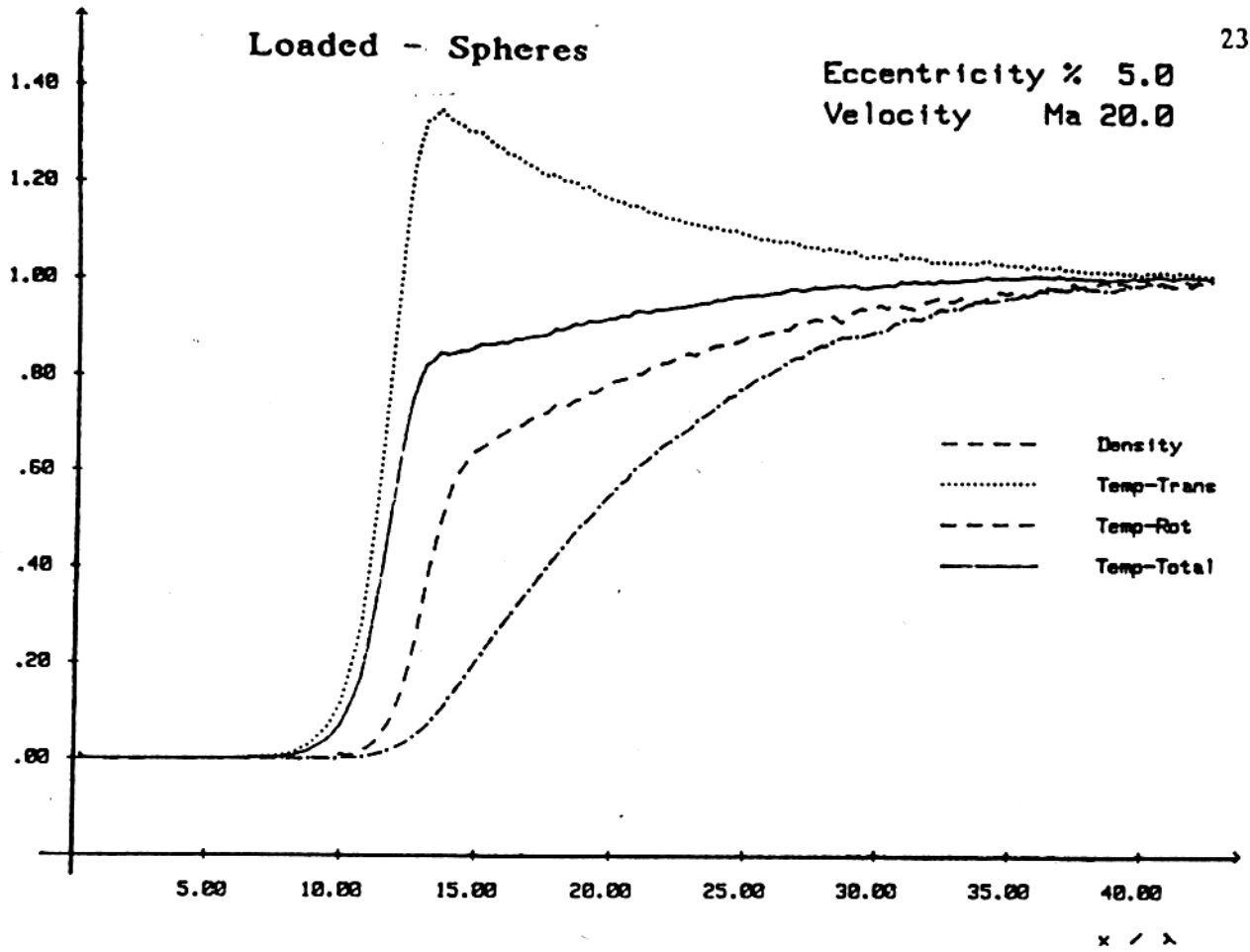
A 'loaded-sphere'-shockwave is similar to a 'phenomenological'-shockwave if the *square of* $\gamma(\varepsilon)$ is proportional to the *collision rate*, provided all other scales of influence (e.g. Mach-Number,...) are unaltered.

For 20 Ma we have the following comparison data:

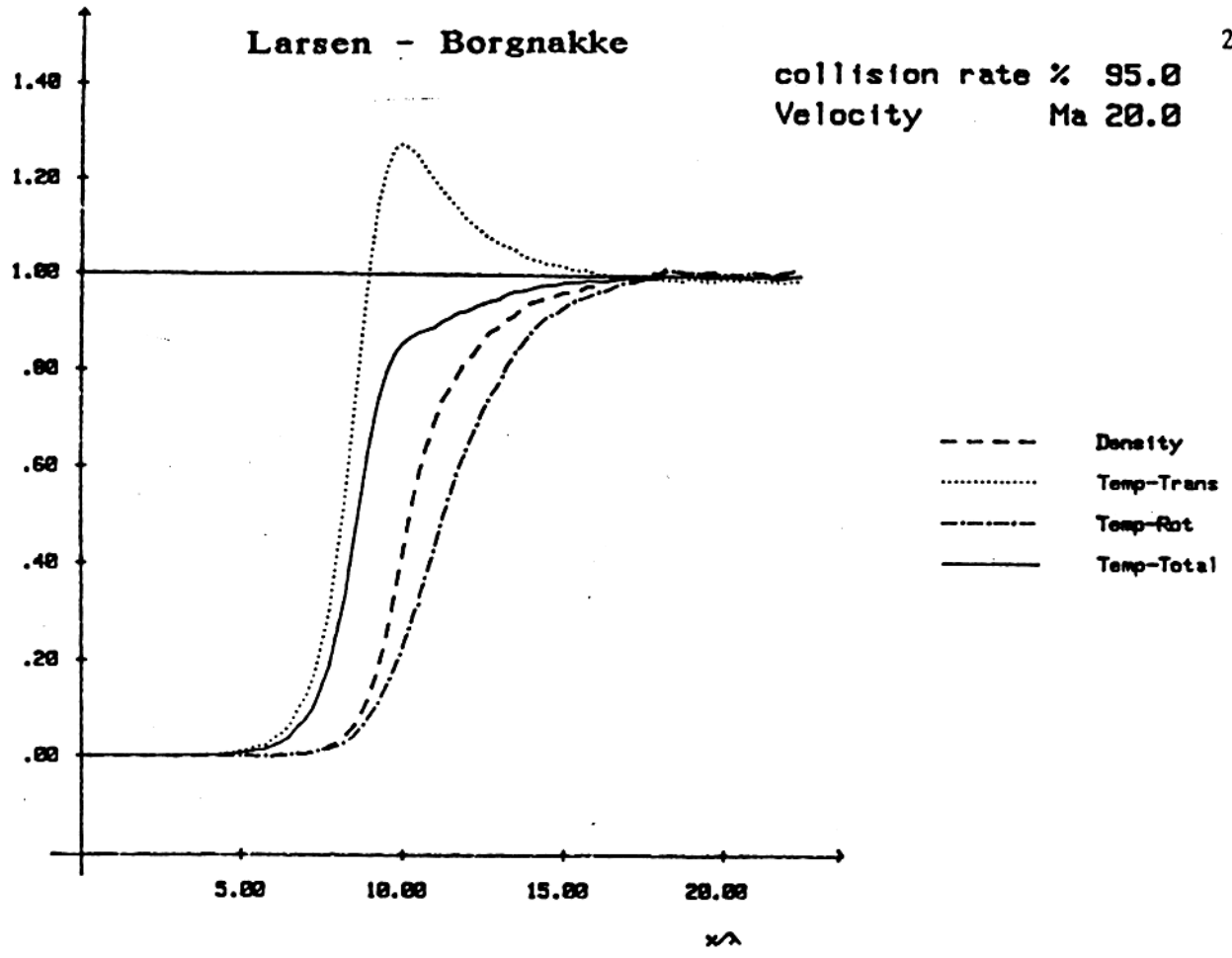| Eccentricity	ε %	5	7,5	10	15	20
Collision Rate	%	98 ~ 99	97	95	90	80

Below the corresponding profiles of the two models are listed. In case of the eccentricities of 5% and 7.5% two comparison profiles of the Larsen-Borgnakke model are shown, while for the other eccentricities the exact corresponding comparison profile are given.

Larsen - Borgnakke

collision rate % 99.0
Velocity   Ma 20.0

- - - - -   Density
....   Temp-Trans
-·-·-·-·-   Temp-Rot
————————   Temp-Total

x ╱ λ

Loaded - Spheres

Eccentricity % 5.0
Velocity   Ma 20.0

- - - - -   Density
....   Temp-Trans
-·-·-·-·-   Temp-Rot
————————   Temp-Total

x ╱ λ

Loaded – Spheres

Eccentricity % 5.0
Velocity Ma 20.0

- - - - Density
.... Temp-Trans
– – – Temp-Rot
——— Temp-Total

x / λ

Larsen – Borgnakke

collision rate % 98.5
Velocity Ma 20.0

- - - - Density
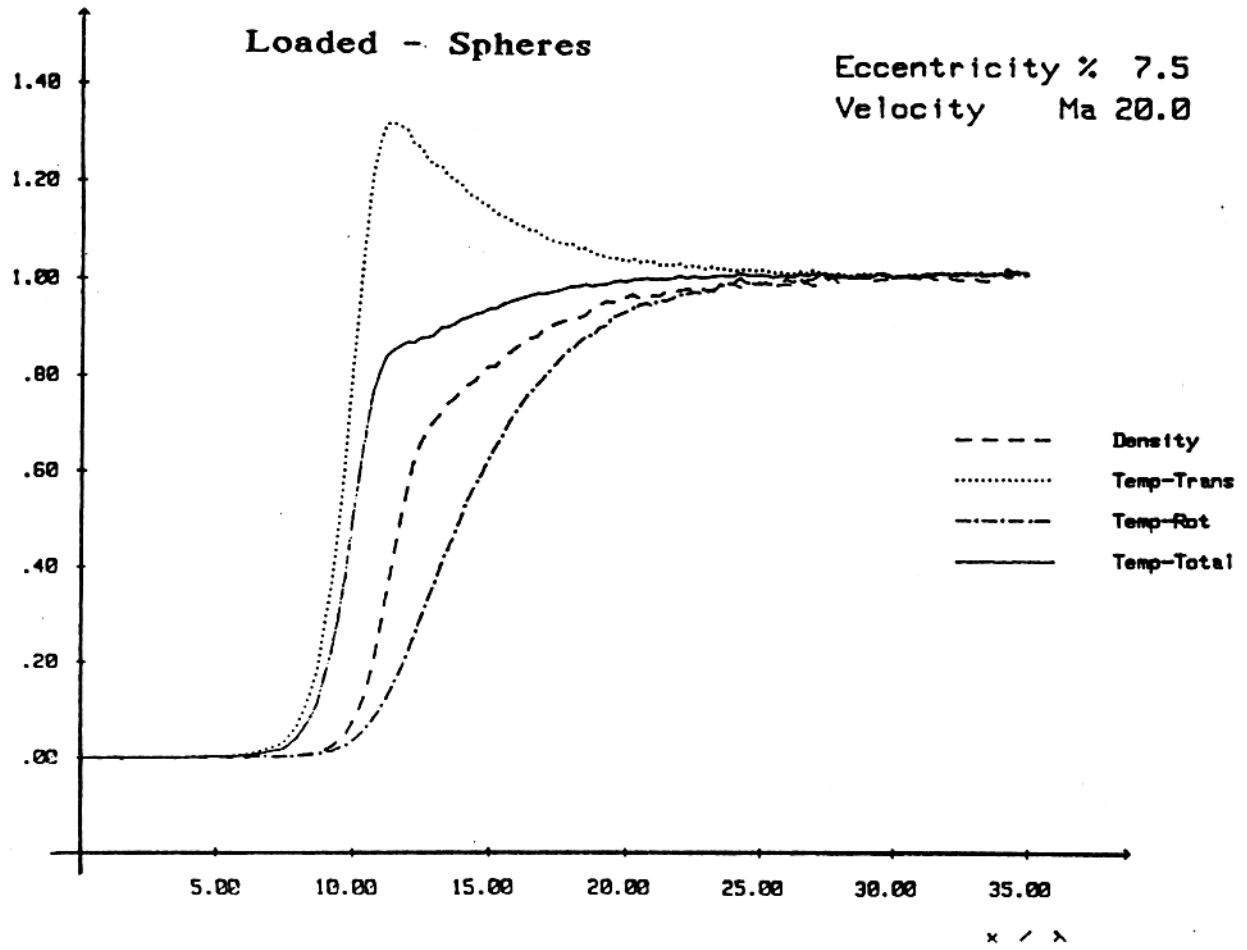........... Temp-Trans
–·–·– Temp-Rot
——— Temp-Total

x / λ

Larsen — Borgnakke

collision rate % 95.0
Velocity   Ma 20.0

- - - -   Density
....   Temp-Trans
-.-.-.-   Temp-Rot
———   Temp-Total

x/λ

Loaded — Spheres

Eccentricity % 7.5
Velocity   Ma 20.0

- - - -   Density
....   Temp-Trans
-..-..-   Temp-Rot
———   Temp-Total

x / λ

Loaded – Spheres

Eccentricity % 7.5
Velocity   Ma 20.0

- – – – Density
- .... Temp-Trans
- –·–·– Temp-Rot
- ——— Temp-Total

x / λ

Larsen – Borgnakke

collision rate % 98.0
Velocity   Ma 20.0

- – – – Density
- .... Temp-Trans
- –·–·– Temp-Rot
- ——— Temp-Total

x / λ

Larsen - Borgnakke

collision rate % 95.0
Velocity   Ma 20.0
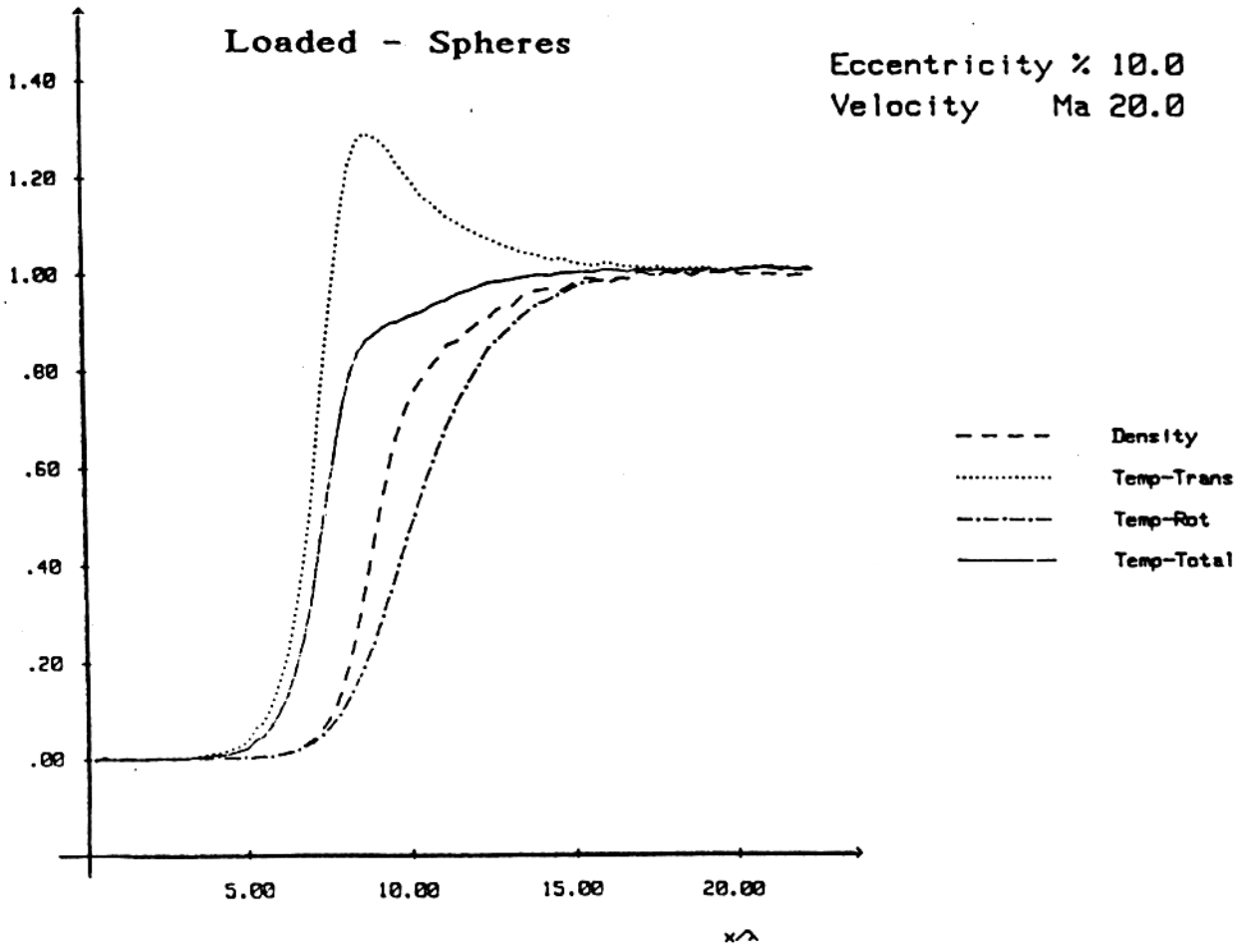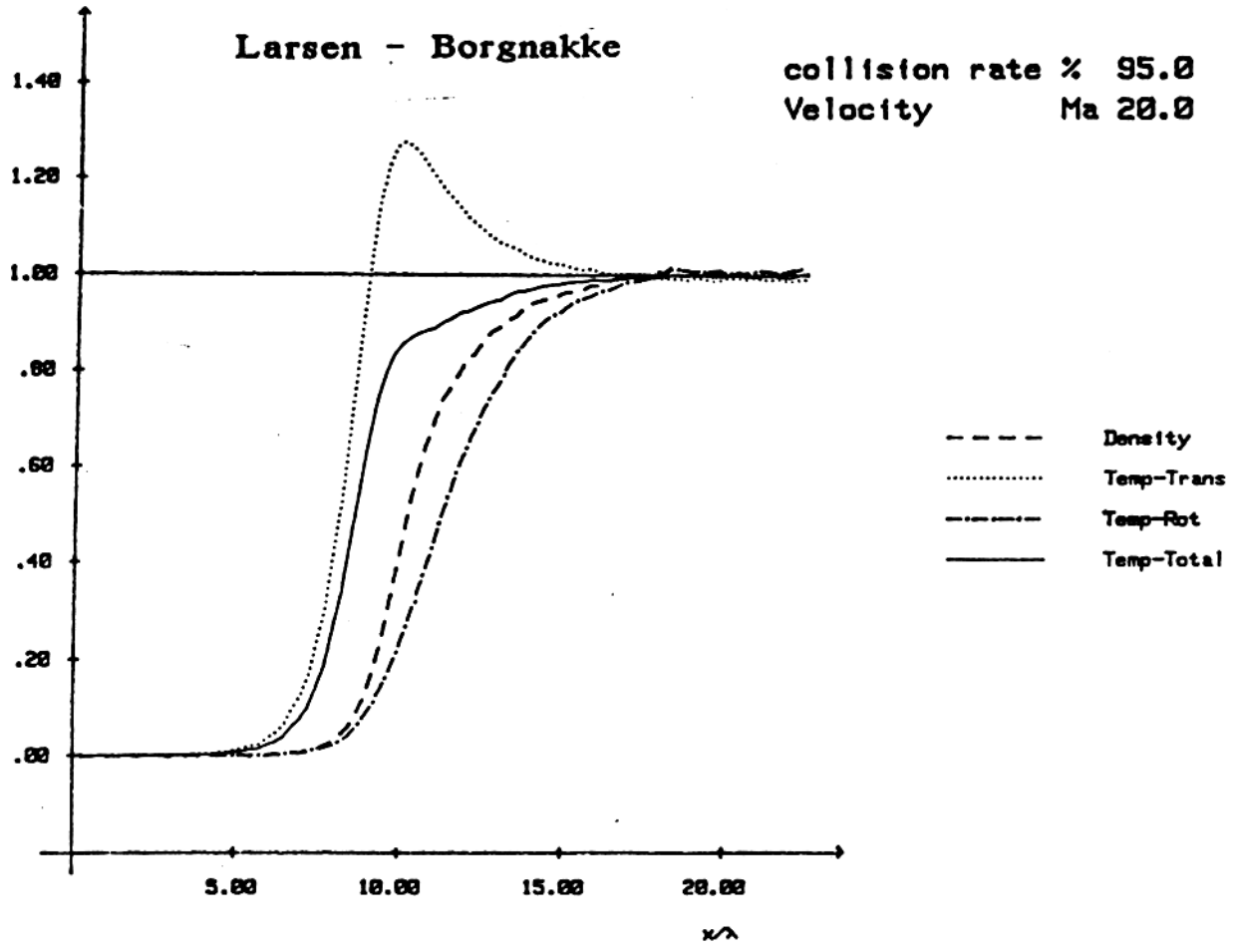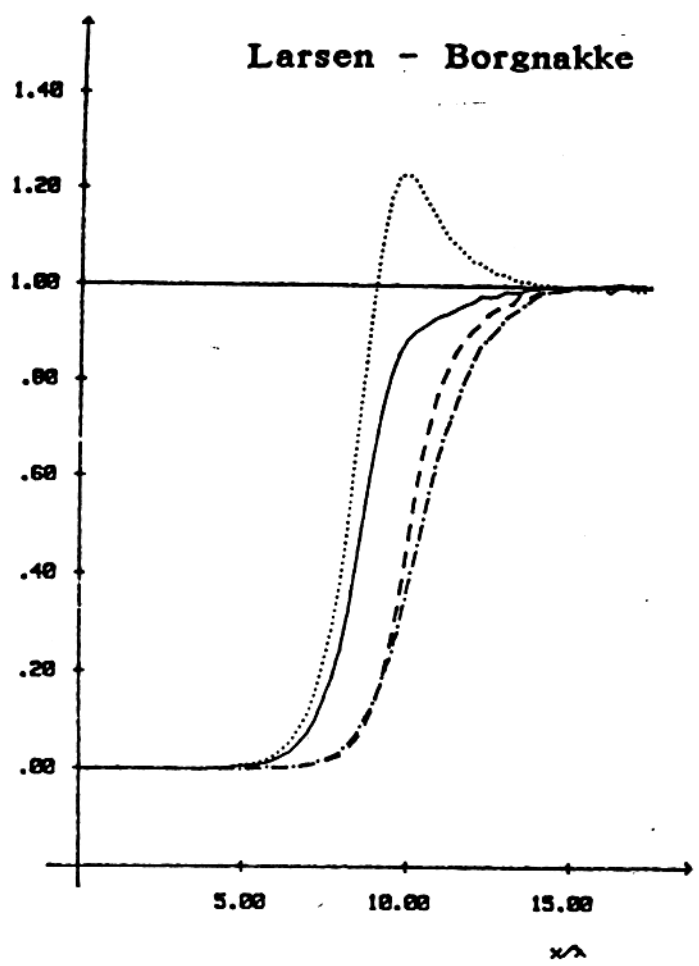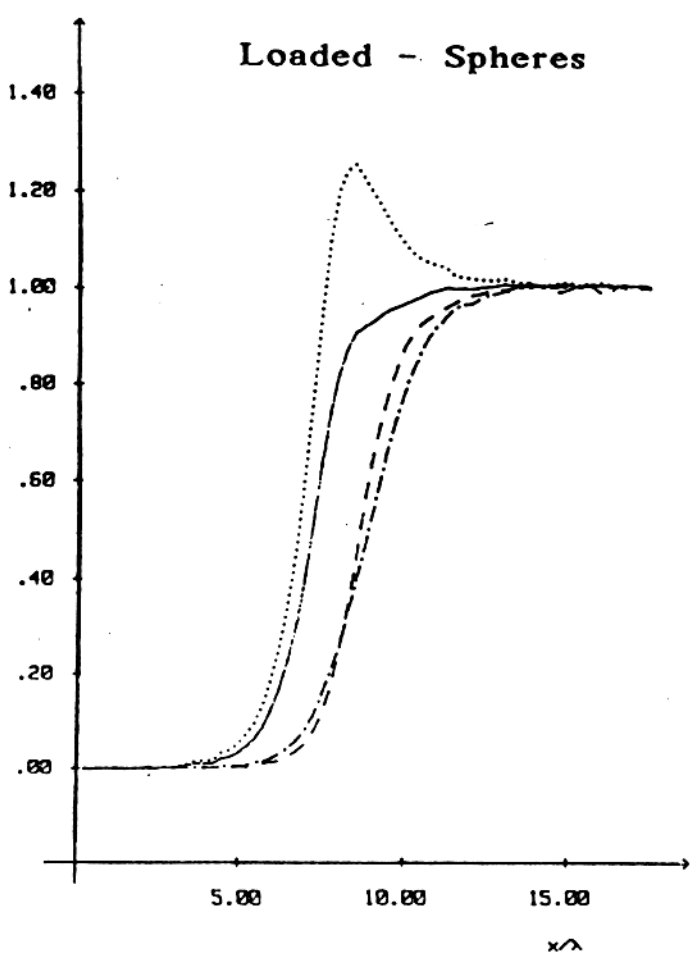
- - - - Density
.... Temp-Trans
-.-.-.- Temp-Rot
——— Temp-Total

Loaded - Spheres

Eccentricity % 10.0
Velocity   Ma 20.0

- - - - Density
.... Temp-Trans
-.-.-.- Temp-Rot
— — Temp-Total

Larsen - Borgnakke

collision rate % 90.0
Velocity   Ma 20.0

1.40
1.20
1.00
.80
.60
.40
.20
.00

5.00   10.00   15.00

x/λ

- - - -   Density
....   Temp-Trans
-·-··-·   Temp-Rot
————   Temp-Total

Loaded - Spheres

Eccentricity % 15.0
Velocity   Ma 20.0

1.40
1.20
1.00
.80
.60
.40
.20
.00

5.00   10.00   15.00

x/λ

- - - -   Density
....   Temp-Trans
-·-··-·   Temp-Rot
————   Temp-Total

Larsen - Borgnakke

collision rate % 80.0
Velocity   Ma 20.0
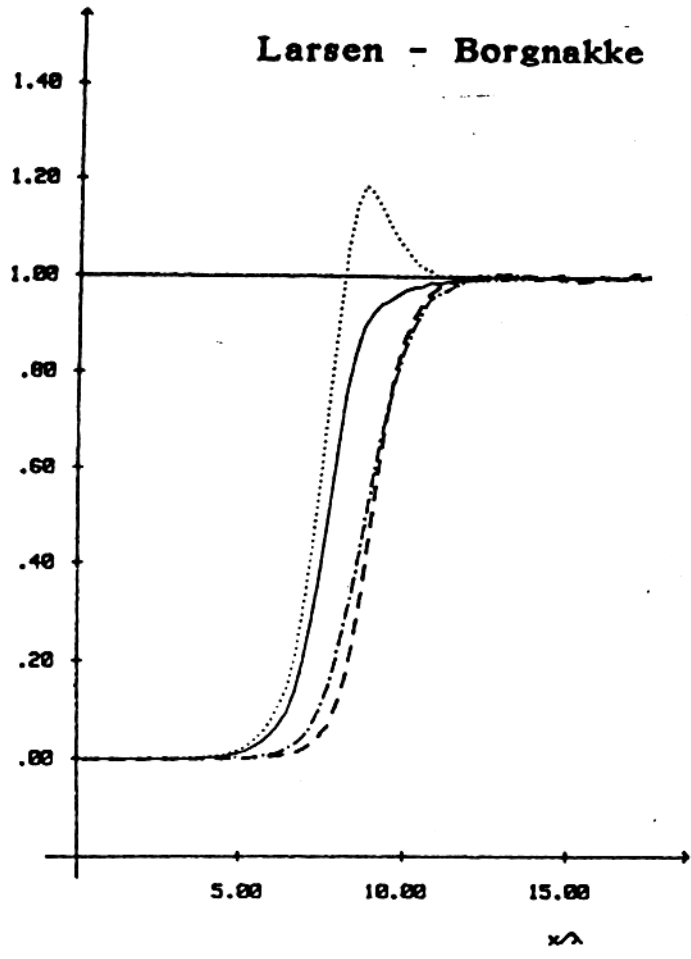
- - - -   Density
.... Temp-Trans
-·-··-·-   Temp-Rot
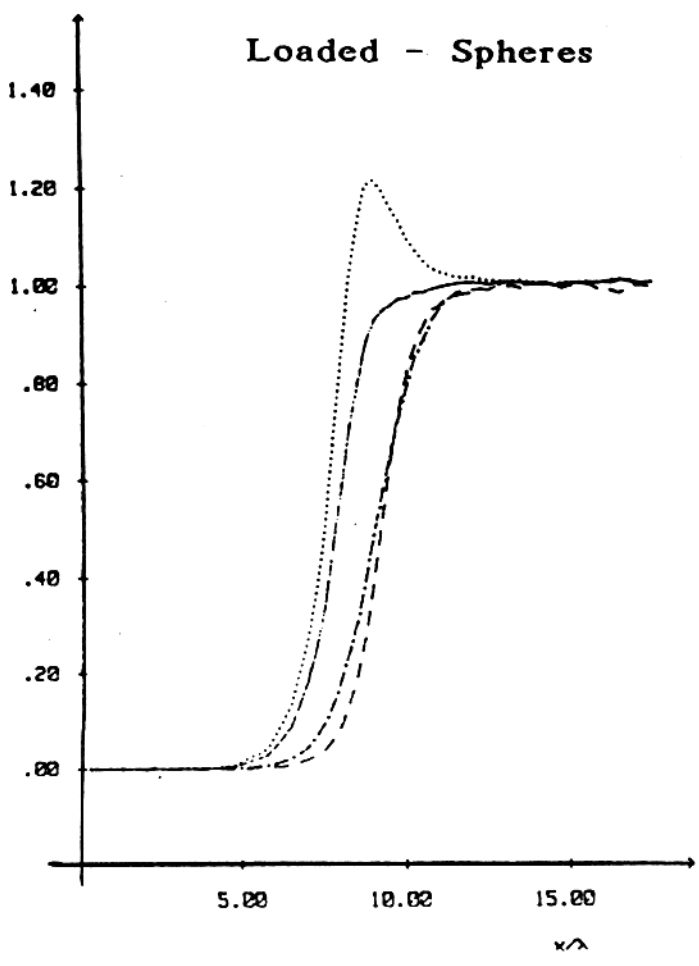————   Temp-Total

Loaded - Spheres

Eccentricity % 20.0
Velocity   Ma 20.0

- - - -   Density
.... Temp-Trans
-·-··-·-   Temp-Rot
—·—·—   Temp-Total

IV) Summary and Conclusions

We developed and implementated two algorithms to solve numerically two different Boltzmann-Equations for gases with internal degrees of freedom. One of those equations and the corresponding algorithm are based on a phenomenological point of view concentrating on the energy exchange between translational and internal modes, the other one starts from a microscopic model which has been described in the first chapter.

Despite the difference both CPU-times and main storage requirements to perform a 1 D shockwave are nearly the same.

	CPU-times in min	main storage
Larsen-Borgnakke	10 $\left(\text{coll. rate} \sim 0.6\right)$ 40 $\left(\text{coll. rate} \sim 1.0\right)$	$\leq$ 12 MB
Loaded-Spheres	14 $\left(\text{eccentricity} \sim 20\,\%\right)$ 40 $\left(\text{eccentricity} \sim 5\,\%\right)$	$\leq$ 15 MB

In all our testcases the density, kinetic and internal temperature profiles are in a good agreement if the corresponding parameters eccentricity and collision rate are chosen in a suitable manner. This result may be interpreted as an additional confirmation of the Larsen-Borgnakke model.

However due to the quite small CPU-times needed to perform 1 D shockwave calculations with the 'loaded-sphere' model we have now a computational tool at hand to study the behavior of a gas of rotating molecules if a strong magnetic field is applied.

References .

[1] Jeans, J.H. : "Dynamical Theory of Gases", Cambridge University Press, New York (1904)

[2] Haight, C.H., Lundgren, T.S. : "Shock Structure in a Gas of Rigid Non-central Particles", The Physics of Fluids, 10 , No 4 (1967)

[3] Körber, S. : "Zur Numerik der Boltzmann-Gleichung Polyatomiger Gase", Thesis, University Kaiserslautern (1990)

[4] Cercignani, C. : "Theory and Application of the Boltzmann-Equation", Scottish Academic Press, London (1975)

[5] Robben, F. , Talbot, L. : Phys. Fluids 9, pp 633 - 653 (1966)

[6] Babovsky, H., Gropengießer, F., Neunzert, H., Struckmeier, J., Wiesen, B. :
"Low Discrepancy for the Boltzmann-Equation",
16th RGD - Symposium: Progr. in Astronautics and Aeronautics
118, pp 85 - 99, American Institut of Aeronautics & Astronautics,
Inc., Washington, D.C. (1989)

[7] Gropengießer, F., Neunzert, H., Struckmeier, J. :
"Computational Methods for the Boltzmann-Equation",
AGTM Report No 43, University Kaiserslautern (1990)

[8] Babovsky, H. : "A Convergence Proof for Nanbu's Boltzmann Simulation Scheme", Eur. Journal of Mechanics 8, pp. 41 - 55 (1989)

[9] Nanbu, K. : "Theoretical Basis of the Direct Monte Carlo Method", Proc. of the 15th RGD - Symposium, Vol. 1, V. Boffi & C. Cercignani eds., pp. 369 - 383 (1986)

[10] Borgnakke, C., Larsen, P.S. : "Statistical Collision Model for Monte-Carlo Simulation of Polyatomic Gas Mixture", Journal of Computational Physics, 18 , pp 405 - 429 (1975)